Food Chemistry: X 22 (2024) 101251

Contents lists available at ScienceDirect

Food Chemistry: X

journal homepage: www.sciencedirect.com/journal/food-chemistry-x

Physicochemical and antimicrobial properties of soy protein isolate films incorporating high internal phase emulsion loaded with thymol

Yuan Zhao [a], Linfan Shi [a,b], Zhongyang Ren [a,b], Qun Liu [a,b], Yucang Zhang [a,b], Wuyin Weng [a,b,*]

[a] *College of Ocean Food and Biological Engineering, Jimei University, Xiamen 361021, China*
[b] *Engineering Research Center of the Modern Technology for Eel Industry, Ministry of Education, Xiamen 361021, China*

A R T I C L E I N F O

Keywords:
Emulsion films
High internal phase emulsion
Physicochemical properties
Thymol
Antimicrobial activity

A B S T R A C T

Oil-in-water (O/W) high internal phase (HIP) emulsion was prepared to investigate its effects on the physicochemical properties and antimicrobial properties of soy protein isolate (SPI)-based films. The particle size and migration degree of oil droplets in the SPI film-forming solution with HIP emulsion and the films were lower than those with conventional O/W emulsion or oil. The SPI-based emulsion films with HIP emulsion containing 30 % oil had the lowest water vapor permeability (1.15×10^{-10} $g{\cdot}m^{-1}{\cdot}s^{-1}{\cdot}Pa^{-1}$), glass transition temperature (40.93 °C) and tensile strength (4.47 MPa), and the highest transparency value (12.87) and elongation at break (160.83 %). The antimicrobial test of the SPI-based emulsion films loaded with thymol showed that the thymol encapsulation efficiency, sustained release effect, and growth inhibition effect on microbes were higher for the films with HIP emulsion than those for the films with O/W emulsion or oil.

1. Introduction

The interest in edible films has increased rapidly due to their abilities of inhibiting moisture migration, gases, and aroma and their properties to carry food ingredients, such as antioxidants, antimicrobials, and flavors (Jorge, Gaspar, Henriques, & Braga, 2023; Wang et al., 2023). Microbial contamination is a major factor that reduces food quality and shelf life during storage and even causes foodborne illness (Zhang et al., 2021). Consumers favor antimicrobial films based on natural biopolymers with antimicrobial agents because the residues of synthetic polymer packaging and the added preservatives have safety risks (Li et al., 2023a). However, the stability and sustained release ability of natural antimicrobial agents are insufficient and usually need to be improved by encapsulation (Shao, Xi, & Weng, 2022). Lipophilic antimicrobial agents are not easily affected by environmental moisture, resulting in their good stability and release properties in edible films (Zhang et al., 2021). Meanwhile, lipophilic phenolic compounds have excellent antimicrobial ability because they can destroy the cell membrane of microbes and cause cell death (Pateiro et al., 2021). Therefore, the preparation and encapsulation strategies of edible films with lipophilic antimicrobial agents have received extensive attention.

Edible films are typically prepared from hydrophilic substances, including protein and polysaccharide (Ajesh, Hasan, Mangaraj, Verma, & Srivastav, 2022). Soy protein isolate (SPI)-based edible films have been extensively studied for their excellent mechanical and gas barrier properties (Zhou et al., 2023). SPI-based edible films are added with antimicrobial agents to enhance their biological activities and expand their application range (Rani et al., 2021). The emulsification or encapsulation of lipophilic antimicrobial agents can improve their compatibility and stability and reduce the adverse effects on the films' structure and properties (Dag, Jung, & Zhao, 2023). A previous study proved that the SPI-based films prepared with conventional oil-in-water (O/W) emulsion contained evenly distributed oil droplets because the pre-emulsified small oil droplets are likely to interact with the SPI (Zhao, Ren, Shi, Zhang, & Weng, 2023a). Therefore, the SPI-based films prepared by adding emulsion loaded with lipophilic antimicrobial agents are expected to improve the antimicrobial and slow-release abilities of the films. High internal phase (HIP) emulsion has attracted considerable interest due to their semi-solid textures and the excellent hydrophobic encapsulation ability of bioactive substances (Gao et al., 2021). However, studies on the SPI-based emulsion films prepared with HIP emulsion are lacking. In particular, the influence of HIP emulsion loaded with antimicrobial agents on the antimicrobial activity of SPI-based emulsion films remains unclear.

Thymol is a lipophilic antimicrobial agent with broad-spectrum antimicrobial activity, which has been widely used as a food

* Corresponding author at: College of Ocean Food and Biological Engineering, Jimei University, Xiamen 361021, China.
E-mail address: wwymail@jmu.edu.cn (W. Weng).

https://doi.org/10.1016/j.fochx.2024.101251
Received 12 December 2023; Received in revised form 19 February 2024; Accepted 21 February 2024
Available online 24 February 2024

preservative (Zhang, Cao, & Jiang, 2022). Dissolving thymol in oil can prevent the crystalline of thymol from disrupting the film integrity (Sharma, Munjal, Sharma, & Sharma, 2023). Moreover, the stability and antioxidant effect of thymol can be improved by loading in the O/W emulsion. (Sedaghat Doost, Van Camp, Dewettinck, & Van der Meeren, 2019). Compared to conventional O/W emulsion, the HIP emulsion with high loading capacity has been used as the carrier of various hydrophobic active substances (Bai et al., 2023; Gao et al., 2021). However, there are few reports on the preparation of antimicrobial films using HIP emulsion loaded with thymol.

Therefore, this study aims to improve the compatibility of oil and thymol in films by emulsification to prepare SPI films with good antimicrobial activity. The effect of HIP emulsion alone and loaded with thymol on the physicochemical properties and antimicrobial activities of the SPI-based films were studied. SPI-based films with conventional O/W emulsion were used as a reference. The present study reveals the difference in the effects of conventional O/W emulsion and HIP emulsion on the properties of SPI-based films. The prepared antimicrobial films can be used as food packaging to reduce the addition of antimicrobial agents.

2. Materials and methods

2.1. Materials

SPI and soybean oil were supplied by Linyi Shansong Products Co., Ltd. (Linyi, China) and Yihai Kerry Arawana Holdings Co, Ltd. (Xiamen, China). Sucrose ester with HLB value of 13 (SE-13) was purchased from Liuzhou Aigefu Food Technology Co., Ltd. (Liuzhou, China). Fluorescein isothiocyanate (FITC) and Nile red were supplied by Aladdin Reagent Co., Ltd. (Shanghai, China). Thymol was supplied by Macklin Biochemical Technology Co., Ltd. (Shanghai, China). *Escherichia coli* (*E. coli*) and *Staphylococcus aureus* (*S. aureus*) specimens were obtained from the College of Ocean Food and Biological Engineering, Jimei University (Xiamen, China). All reagents used were of analytical grade.

2.2. Preparation of emulsion

SE-13 (0.1 or 0.4 g) was dissolved in the distilled water (20 or 5 mL) at 70 °C, mixed with soybean oil (5 or 20 g), and homogenized at 15,000 rpm for 3 min using a FJ-200 high-speed homogenizer (Shanghai Specimen Model Factory, China) to prepare O/W and HIP emulsions. The added SE-13 was 2 % of the oil content.

2.3. Preparation of SPI-based emulsion films

A film-forming emulsion (FFE) was prepared following the method of Zhao et al. (2023a). The glycerol (2.25 g) and SPI (9 g) were dispersed in distilled water (100 mL), and heated at 70 °C for 30 min to prepare the SPI solution. Then, the O/W or HIP emulsions were mixed with the SPI solution to prepare the FFE at homogenization conditions of 7,000 rpm for 2 min, and the oil content of FFE was 10 %, 20 % and 30 % (w/w) of SPI, respectively. The FFE without oil and directly added with 1.8 g (20 %, oil/SPI, w/w) of oil was used as the control group. The FFE was spread on the rimmed silicone resin plate to dry at 25 °C and 50 % relative humidity to obtain SPI-based emulsion films, which were then stored under the same conditions until analysis.

On the basis of the pre-experiment results, the emulsion films with 20 % (oil/SPI, w/w) oil content were selected to prepare antimicrobial films using the above methods. The oil solution of thymol with concentrations of 25 %, 50 %, and 75 % (w/w) was used to prepare O/W and HIP emulsions. The films with thymol were prepared using the above emulsion, and the FFE contained 5 %, 10 %, and 15 % (thymol/SPI, w/w) of thymol, respectively. The control group FFE with 0.9 g (10 %, thymol/SPI, w/w) of thymol was prepared using 50 % thymol oil solution.

2.4. Confocal laser scanning microscope (CLSM) observation

The CLSM images of emulsion, FFE and SPI-based emulsion films were captured using a TCS-SP8 CLSM (Leica, Germany). The emulsion, FFE, and emulsion films were stained by FITC solution and Nile red solution as previously reported (Zhao, Ren, Shi, & Weng, 2023b). The protein and oil were detected using laser sources excited at 488 and 552 nm. The diameter distribution of the oil was analyzed by particle size analysis software (Nano measurer 1.2).

2.5. Scanning electron microscope (SEM) observation of films

The cross-sectional morphology of SPI-based emulsion films were observed using a Phenom ProX G6 SEM (Thermo Fisher Scientific Inc., USA) following the method of Zhao et al. (2023a) at a magnification of 2500 ×. The film sample fragments were obtained by fracturing the SPI-based emulsion films in liquid nitrogen and drying them with silica gel before measurement.

2.6. Fourier transform infrared (FTIR) spectroscopy of films

The FTIR spectra of SPI-based emulsion films were measured using a Nicolet iS50 FTIR spectrometer (Thermo Fisher Scientific Inc., USA) at room temperature (Xue, Gu, Wang, Li, & Adhikari, 2019). The measurement range, number of scans, and resolution were 4000–800 cm^{-1}, 32, and 4 cm^{-1}, respectively.

2.7. Differential scanning calorimetry (DSC) of films

The DSC thermograph of SPI-based emulsion films (2 mg) was measured using a Q2000 DSC (TA Instrument, USA) following the reports of Hu et al. (2023). The test range and heating rate of DSC was 10 °C − 100 °C and 5 °C/min, respectively.

2.8. Mechanical properties of films

The mechanical properties of SPI-based emulsion films were evaluated using a TA-XT Plus texture analyzer (Stable Micro System, UK) (Zhao et al., 2023b). The thicknesses of the sample strips (20 mm × 45 mm) were measured using a handheld micrometer thickness gauge (Ozaki Mfg. Co., Tokyo, Japan), and the average thickness was calculated by three random points.

2.9. Water vapor permeability (WVP) of films

The WVP of SPI-based emulsion films was evaluated as previously described (Kaewprachu et al., 2018). Dried silica gel was added to the cups (0 % RH) and covered with the film samples, then placed the cups in a closed environment (100 % RH, 30 °C) with distilled water. The upper surfaces of the film samples were in contact with the 100 % RH side. The cup weight was measured every hour for 9 h. The WVP of films was calculated as follows:

$$WVP\ \left(gm^{-1}s^{-1}Pa^{-1}\right) = \frac{W \times x}{A \times t \times \Delta p}$$

where *W, x* and *A* are the cup weight of gain (g), the film thickness (m), and the covered area of the film (m^2), *t* is the time interval (s), and Δp is the vapor pressure difference on both sides of the film (Pa).

2.10. Color and opacity of films

The color of SPI-based emulsion films was evaluated using an YS-3010 spectrophotometer (Shenzhen Threeenh Technology Co., Ltd., China). The standard plate was used as a background ($L^* = 91.86$, $a^* = -0.88$, $b^* = 1.42$) to measure the L^*, a^*, and b^* values of the films, and the total color difference (ΔE) was computed as reported by Zhou et al. (2021).

The opacity of SPI-based emulsion films was determined using a UV-8000A UV–visible spectrophotometer (Shanghai Yuanxi Instrument Co., China) at a wavelength of 600 nm (Hu et al., 2022). The opacity of films was calculated as follows:

$$\text{Transparency value} = \frac{A_{600}}{x}$$

where A_{600} is the absorbance at 600 nm and x is the film average thickness (mm). A high transparency value indicates a high level of opacity.

2.11. Encapsulation efficiency (EE) of thymol

Film samples (approximately 100 mg) were placed in 35 mL glass vials with hexane (20 mL) and shaken overnight at 25 °C. The amount of thymol entrapped in the film samples was calculated against the absorbance of the mixed solution at 275 nm and the standard curve. The initial amount of thymol in the film samples was determined from the amount of thymol in the FFE. The EE of thymol was calculated using the following formula (Liang & Gao, 2023):

$$EE\ (\%) = \frac{m_1}{m_0} \times 100$$

where m_0 and m_1 are the initial amount of thymol in the film samples (g) and the amount of thymol entrapped in the film samples (g).

2.12. Thymol release properties

The thymol release properties of SPI-based emulsion films in water and 50 % (v/v) ethanol–water solution were investigated following a previous method (Lian, Shi, Zhang, & Peng, 2020) with some modifications. Film samples (20 mm × 45 mm) were soaked in water or 50 % ethanol solution (40 mL) at 25 °C for 24 h. Afterward, 3 mL of the mixed solution was taken at a fixed time, and its absorbance was measured at 275 nm. The same volume of water or 50 % ethanol solution was added after every removal of the mixed solution. Thymol release was calculated against the standard curve, and the accumulative thymol release (%) was calculated as the following formula:

$$\text{Accumulative thymol release } (\backslash\%)) = \frac{m_2}{m_1} \times 100$$

where m_1 and m_2 are the amount of thymol entrapped in the film samples (g) and the amount of thymol released into the solvent (g).

2.13. Antimicrobial properties of films

The SPI-based emulsion films' antimicrobial properties were evaluated by the disk agar diffusion method (Almasi, Radi, Amiri, & McClements, 2021). *E. coli* and *S. aureus* were used as the bacteria for the experiment. All experimental instruments and tools were treated with ethanol before the preparation of film samples. The film sample disks (6 mm, approximately 10 mg) were prepared aseptically and placed on solidified agar plates previously inoculated with 100 μL of 10^6 CFU/mL activated bacterial suspensions. The agar plates were then incubated (37 °C, 24 h), and the inhibition zone diameter of the film sample disks was measured.

2.14. Statistical analysis

Measurements were performed in triplicate for each test. The data were analyzed by one-way analysis of variance and Duncan's test at $P < 0.05$ using the SPSS statistical analysis computer program (SPSS Inc., USA).

3. Results and discussion

3.1. CLSM images of emulsions and FFE

As presented in Fig. 1a and b, the distribution and droplet size of oil in the emulsion and FFE were characterized by CLSM. The red droplets were sparsely dispersed in the green O/W emulsion matrix but were packed closely and almost completely fused together with the green HIP emulsion matrix. In general, a successfully prepared HIP emulsion has 5 %–50 % surfactant (Bai et al., 2023). In this study, a HIP emulsion was successfully prepared using 2 % sucrose ester. This phenomenon occurred because the key factors of stable HIP emulsion-like vesicles can form in aqueous solution when the concentration of sucrose esters is higher than the critical aggregation concentration, and the vesicles of sucrose esters were reported in a previous study (Hu, Binks, & Cui, 2021).

Large and unevenly distributed oil droplets were observed in the FFE homogenized by directly adding 20 % oil (control 20). By comparison, small oil droplets were found in the FFE added with O/W and HIP emulsions (Fig. 1a), indicating that the emulsified oil is easier to disperse into FFE than oil. The oil droplets were larger and easier to flocculate in the FFE with O/W emulsion than those in the FFE with HIP emulsion, and this phenomenon became highly evident with the increase in oil content (Fig. 1b). The speculation of FFE preparation process is illustrated in Fig. 1c according to the above results. The sucrose ester in the O/W emulsion can reduce the interfacial tension and prepare FFE with middle particle size oil droplets. On the other hand, the HIP emulsion contains vesicles can form a protective layer around the oil droplets, resulting in the prepared FFE with small particle size oil droplets.

3.2. Physicochemical properties of SPI-based emulsion films

3.2.1. CLSM images of SPI-based emulsion films

The oil droplet size in the SPI-based emulsion films is exhibited in Fig. 2a and c. The control groups had the largest oil droplets, followed by the SPI-based emulsion films with O/W and HIP emulsions. This finding was consistent with the size order of oil droplets in the FFE (Fig. 1a). The SPI-based emulsion films contained larger oil droplets compared to the FFE, regardless of the oil content (Fig. 1a and 2a). This suggested that the oil droplets coalesce easily during drying (Fattahi & Seyedain-Ardabili, 2021). Meanwhile, the coalescence of the SPI-based emulsion films with HIP emulsion was not evident compared with those directly added with oil and O/W emulsion. This phenomenon suggested that using HIP emulsion could effectively prevent oil coalescence during film formation and the preparation SPI-based emulsion films with evenly distributed oil droplets.

3.2.2. SEM images of SPI-based emulsion films

Fig. 2b shows that the compact and smooth cross-section structure of the SPI films became rough and uneven with the addition of oil or emulsion. Therefore, the added emulsion can destroy the compactness of the emulsion film structure, which was consistent with the effect of Pickering emulsion on konjac glucomannan film structure (Xu et al., 2023). The decreased structural compactness of the SPI films was due to the hindrance of protein–protein interactions by the dispersed oil droplets in the protein network (Hu et al., 2022). The SPI-based emulsion films with HIP emulsion exhibited the smallest oil droplets, as observed in the CLSM images (Fig. 2a). Moreover, the SPI-based emulsion films directly added with oil showed the most evident oil droplet flotation and even had oil layers forming on the upper surface. With the increase in oil content, there was a continuous increase in the degree of oil droplet flotation to the upper surface in SPI-based emulsion films with O/W emulsion. Meanwhile, the evenly dispersed oil droplets were observed in the SPI-based emulsion films with HIP emulsion. Therefore, the degree of oil droplet flotation is related to the oil droplet size because small oil droplets have a large total surface area, allowing them to

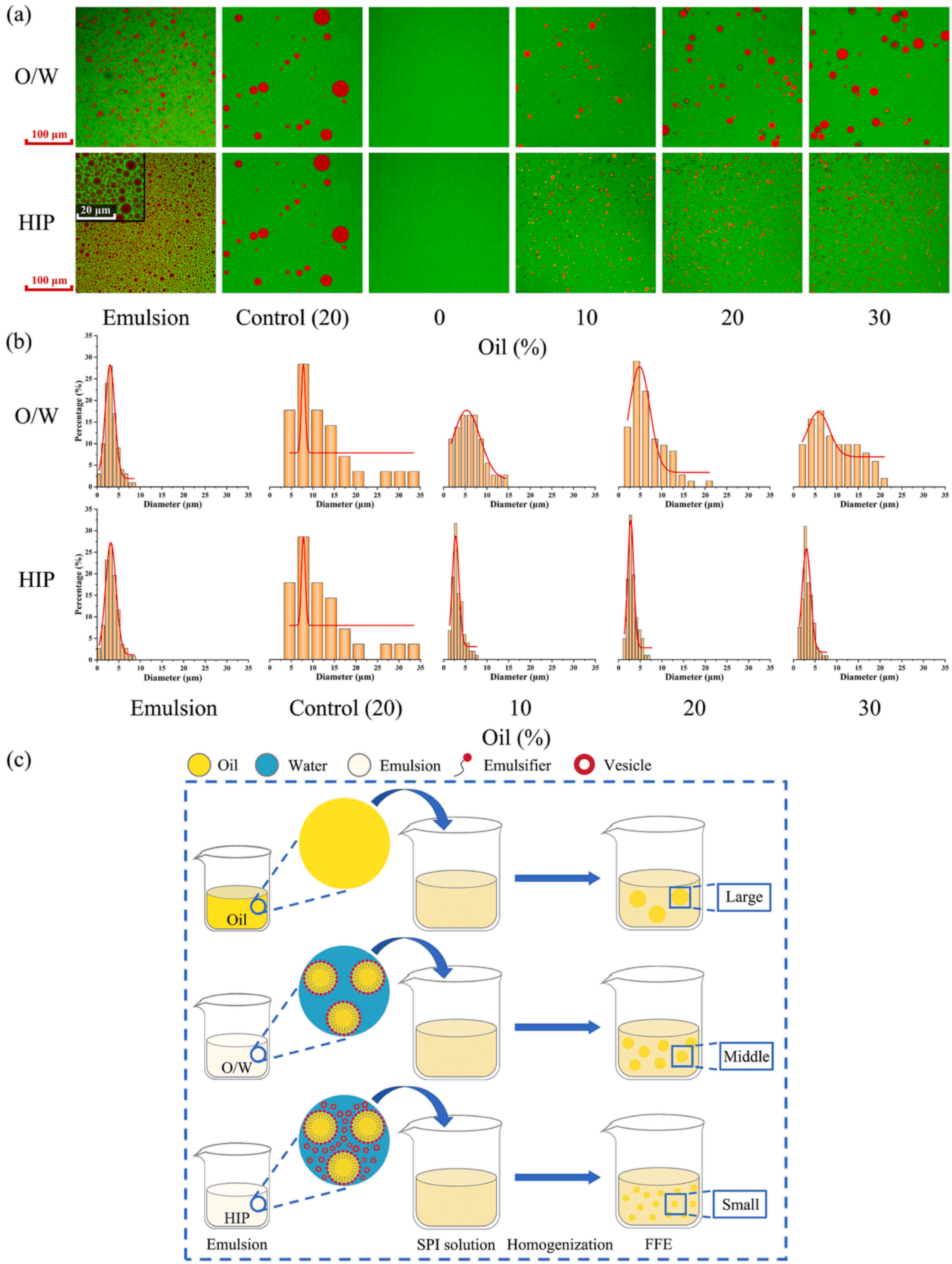

Fig. 1. (a) Confocal laser scanning microscope (CLSM) images of emulsion and film-forming emulsion (FFE); (b) Oil particle size distribution of emulsion and FFE; (c) Schematic of the preparation of FFE with oil, oil-in-water (O/W) emulsion, and high internal phase (HIP) emulsion.

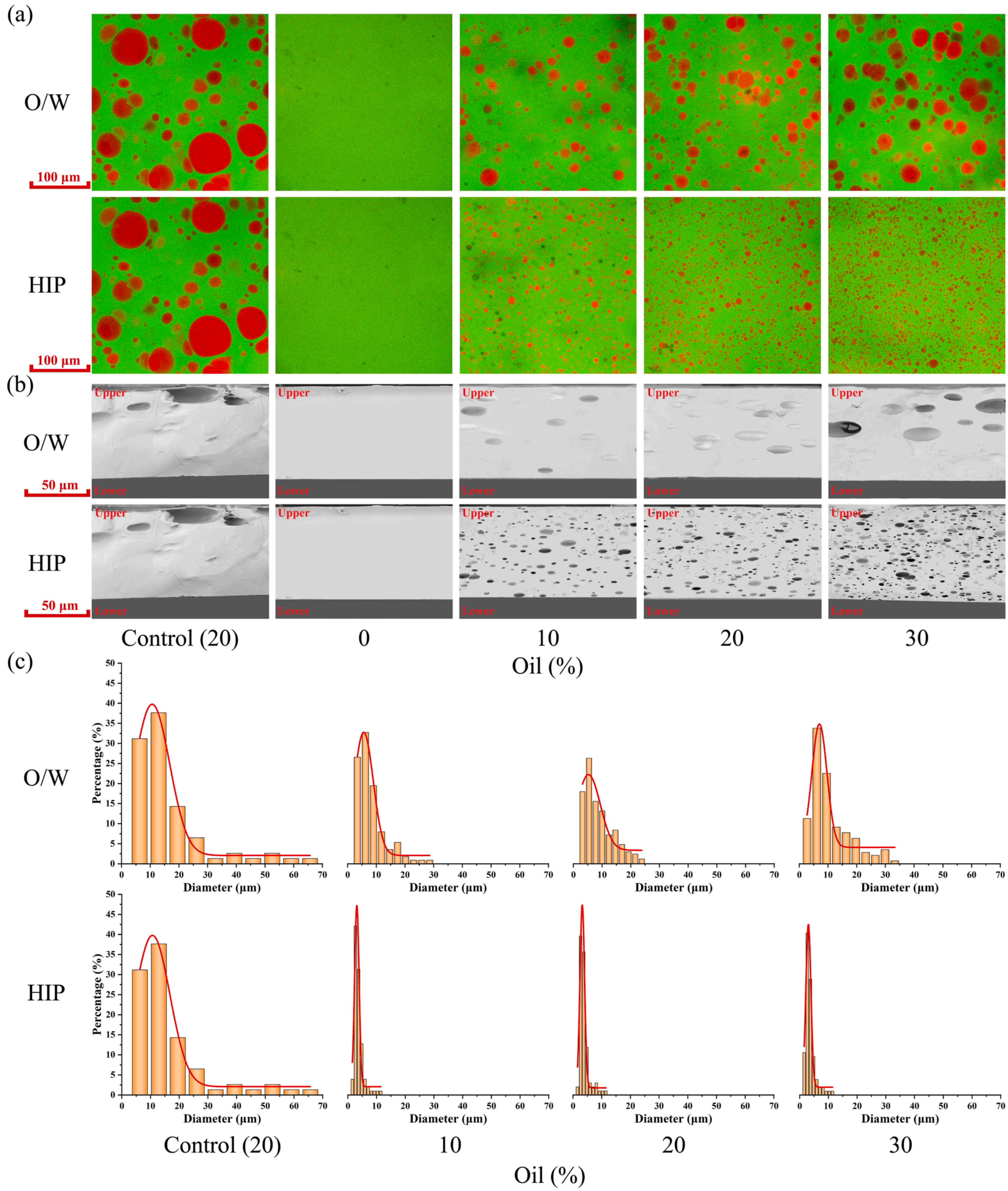

Fig. 2. (a) CLSM images of soy protein isolate (SPI)-based emulsion films; (b) Cross-sectional microstructure of SPI-based emulsion films; (c) Oil particle size distribution of SPI-based emulsion films.

interact effectively with the protein gel network (Li et al., 2022). Similar results were reported in a study on the preparation of emulsion films with different homogenization conditions (Fattahi & Seyedain-Ardabili, 2021).

3.2.3. FTIR analysis of SPI-based emulsion films

FTIR was performed to investigate the intermolecular interaction and content of each component in SPI-based emulsion films. Amide I (1632 cm^{-1}), amide II (1532 cm^{-1}) and amide III (1236 cm^{-1}) were related to the C═O stretching vibration, N—H bending vibration) and C—N stretching vibration, respectively, which represented the SPI characteristic absorption peaks (Xue et al., 2019). The wavenumber at 3273 cm^{-1} (N—H stretching vibration/O—H stretching vibration) and 1743 cm^{-1} (C═O stretching vibration) are the amide A and soybean oil characteristic peaks, which can be used to characterize changes in hydrogen bonding and oil content (Ozulku, Yildirim, Toker, Karasu, & Durak, 2017, Zhou et al., 2023).

As presented in Fig. 3a and b, the characteristic peak intensity of oil was higher on the upper surface of the SPI-based emulsion films with oil or O/W emulsion compared to the lower surface. No difference in oil characteristic peak intensity was observed between two side surfaces of the SPI-based emulsion films with HIP emulsion (Fig. 3a and b). When the added oil content was 20 %, the SPI-based emulsion films directly added with oil had the highest oil characteristic peak intensity on the upper surface, followed by those in the SPI-based emulsion films with O/W and HIP emulsions. The lower surface of the films had an opposite order of oil characteristic peak intensity. This result indicated that the oil droplets easily migrate upward more easily in the SPI-based emulsion films directly added with oil, but not in the SPI-based emulsion films with HIP emulsion. This finding was consistent with the longitudinal distribution of oil in the SEM images (Fig. 2b). By contrast, the peak intensities of amide I, amide II, and amide III on the surface decreased with the increasing peak intensity of oil in all SPI films (Fig. S1). This phenomenon can be attributed to the replacement of protein with the accumulated oil, leading to the low homogeneity of films (Zhao et al., 2023b). Meanwhile, the addition of oil affected the hydrogen bonding interactions formed by protein–water and protein–protein, resulting in the peak intensity of amide A decreased with the increasing characteristic peak intensity of oil (Hu et al., 2023).

3.2.4. DSC analysis of SPI-based emulsion films

Fig. 3c and d present the DSC thermograph and glass transition temperature (T_g) of the SPI-based emulsion films. The T_g of the SPI films was 58.13 °C, which decreased with the addition of oil or emulsion. In general, oil incorporation can interrupt protein–protein interactions and increase the chain mobility of polymer chains (Tongnuanchan, Benjakul, & Prodpran, 2014), resulting in a lower T_g of the films. In this study, oil incorporation had the least effect on the T_g of SPI films, followed by the incorporation of O/W and HIP emulsions. Moreover, the content of O/W emulsion had no significant effect on the T_g of the SPI-based emulsion films ($P > 0.05$), and the increase in HIP emulsion content decreased the T_g of SPI-based emulsion films. This phenomenon can be attributed to

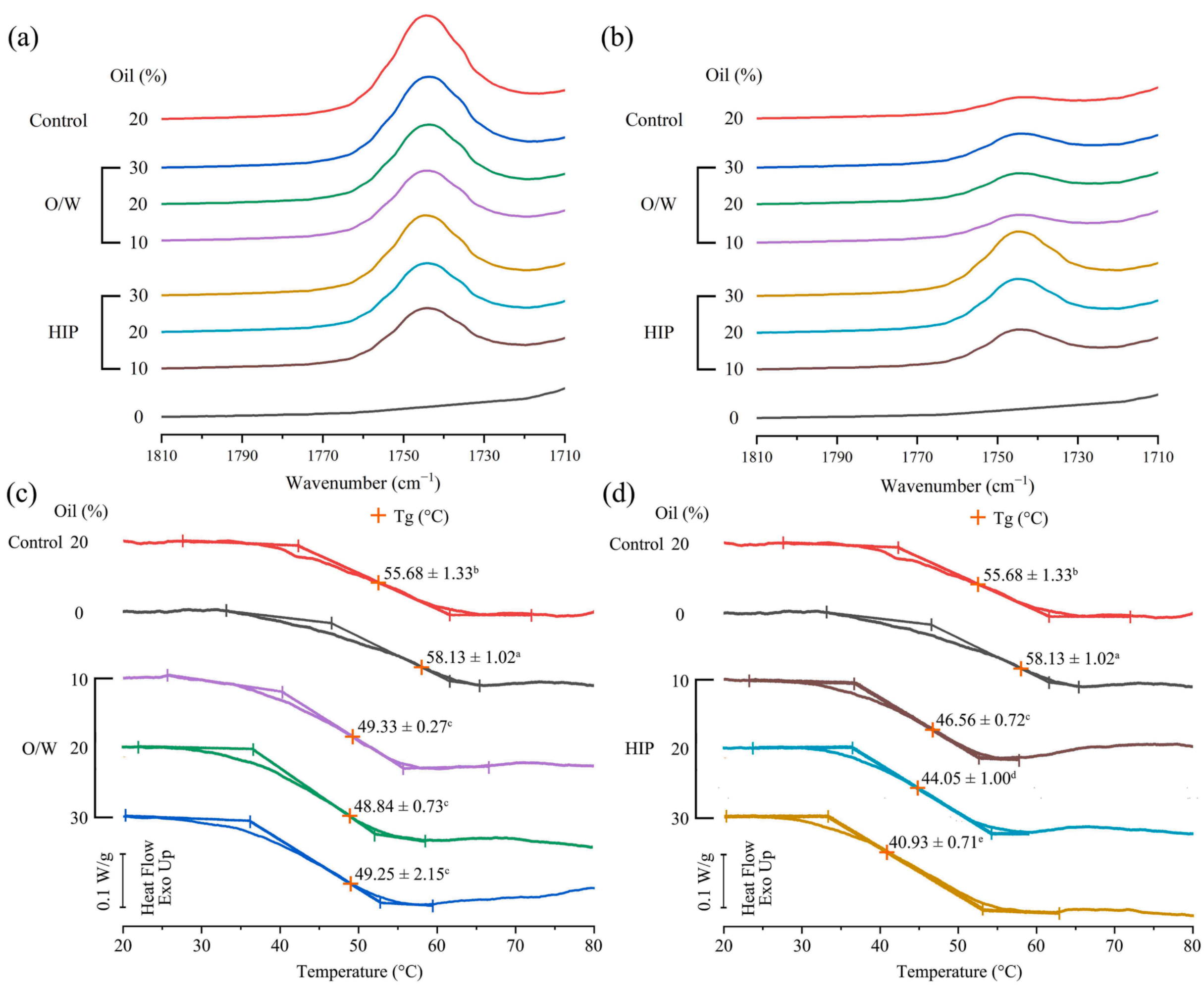

Fig. 3. Fourier transform infrared spectra of oil characteristic peaks (a: upper surface, b: lower surface) of SPI-based emulsion films; Differential scanning calorimetry thermograph of SPI-based emulsion films with O/W emulsion (c) and HIP emulsion (d).

the plasticizing effect of oil in the films (Rashid et al., 2023), which is usually enhanced by the increasing oil content. However, the SPI-based emulsion films with O/W emulsion presented phase separation whose degree increased with the oil content (Fig. 2b). The upward migration of the oil in the SPI-based emulsion films decreased its content between the protein chains, resulting in a reduced plasticizing effect of oil. However, the plastization of small oil droplets is better than that of large oil droplets (Zhao et al., 2023a). Therefore, the addition of HIP emulsion could effectively improve the mobility of the polymer chains in SPI films.

3.2.5. Mechanical properties of SPI-based emulsion films

As presented in Table 1, the SPI films had the highest tensile strength (TS; 7.56 MPa) and lowest elongation at break (EAB; 50.08 %). The TS of the SPI films significantly decreased with the incorporation of oil or emulsion ($P < 0.05$) and further decreased with the increasing oil content regardless of the incorporation strategies. Introducing oil hinders the hydrogen bonding interactions between protein molecules (Hu et al., 2023), and the effect becomes highly pronounced as the oil content increases (Fig. S1). The TS of the SPI-based emulsion films directly added with oil was the closest to that of the SPI films, followed by the SPI-based emulsion films with O/W and HIP emulsions. The coalescence and migration of oil droplets prevent them from being effectively incorporated into the protein network structure, thus reducing their effect on the protein network. The added oil or emulsion increased the EAB of the SPI films (Table 1) because oil increased the chain mobility of protein chains in the SPI films (Tongnuanchan et al., 2014). However, the upward migration of oil in the films led to a reduced plasticizing effect. Thus, the EAB of the SPI-based emulsion films directly added with oil was smaller than that of the SPI-based emulsion films with O/W or HIP emulsions. Meanwhile, the EAB of the SPI-based emulsion films with HIP emulsion increased with the oil content, but this phenomenon was not founded in the SPI-based emulsion films with O/W emulsion. The above results were consistent with the DSC analysis (Fig. 3c and d).

3.2.6. WVP of SPI-based emulsion films

WVP is an important index of films for food packaging applications because the loss and absorption of moisture in food system can lead to alterations in food quality and shelf life (Zhang, Zhang, Mujumdar, Wang & Ma, 2023). As presented in Table 1, the WVP of the SPI films was 2.72×10^{-10} g·m^{-1}·s^{-1}·Pa^{-1}, which was higher than that of gelatin films (1.65×10^{-10} g·m^{-1}·s^{-1}·Pa^{-1}; Kaewprachu et al., 2018) and cellulose–wheat gluten composite films (1.63×10^{-10} g·m^{-1}·s^{-1}·Pa^{-1}; Shen et al., 2022). The poor water vapor barrier capacity of protein films can be enhanced by incorporating oil and further enhanced by reducing the oil droplet size (Li, Sha, Yang, Ren, & Tu, 2023b). In this study, the WVP of the SPI-based emulsion films decreased with the increase in oil content. Moreover, the SPI-based emulsion films with HIP emulsion contained small and evenly distributed oil droplets, resulting in their lower WVP than that of the SPI-based emulsion films with O/W emulsion. The small oil droplets can be widely distributed in the film matrix under the same oil content, resulting in significant water vapor resistance. This phenomenon has been observed in a study on the preparation of emulsion films with different homogenization conditions (Fattahi & Seyedain-Ardabili, 2021). However, the WVP of the SPI-based emulsion films directly added with oil was lower than that of the SPI-based emulsion films with both emulsions. This phenomenon can be attributed to the large oil droplets continuously floating upward and forming oil layers on the upper surface of films (Fig. 2b). Oil tends to agglomerate and migrate upward under low-speed homogenization to form a pseudo-bilayer film. This pseudo-bilayer structure can provide good water vapor resistance (Hosseini, Mousavi, & McClements, 2023).

3.2.7. Color and transparency of SPI-based emulsion films

As presented in Table 2, the SPI films showed the highest L^* (91.67) and a^* values (−1.37) and the lowest b^* value (8.49). With the increase in the oil content, the L^* value decreased and the a^* and b^* values increased, indicating that the films became darker and more yellow. When the oil content was 20 %, the highest L^* value was found in SPI-based emulsion films with direct oil addition, followed by the SPI-based emulsion films with O/W and HIP emulsions. The opposite order was founded for the b^* value. This result indicated that the coalescence and upward migration of oil increased the L^* value and decreased the b^* value. The coalescence and upward migration of oil increased the roughness of the film surface, which led to the decrease the L^* value (Galus, 2018). Meanwhile, the accumulation of soybean oil with a high yellowness led to an increase in b^* value. The ΔE difference of films suggested that the high oil content, small oil droplet size, and evenly distributed oil led to the high difference of color between the films and standard whiteboard.

As shown in Table 2, the increase in oil content significantly increased the transparency value of the films ($P < 0.05$). This finding can be explained by the light scatterings effect of oil in films (Zhou et al., 2021). The small and uniform distribution of oil led to multiple light scattering in the film matrix, and increased transparency values of the SPI-based emulsion films (Zhao et al., 2023a). High transparency values represent low transparency. Therefore, the SPI-based emulsion films with HIP emulsion presented lower transparency than the SPI-based emulsion films with O/W emulsion and those directly added with oil.

3.3. Antimicrobial properties of SPI-based emulsion films

3.3.1. EE of thymol in SPI-based emulsion films

As shown in Fig. 4a, the highest EE of thymol was founded in the SPI-based emulsion films with HIP emulsion, followed by the SPI-based emulsion films with O/W emulsion and those directly added with oil. Dissolving thymol in high oleic sunflower oil and preparing O/W emulsion can help inhibit its recrystallization and improve its stability; small oil droplets are beneficial to further improve the solubility and stability of thymol (Sedaghat Doost et al., 2019). The migration degree of oil may affect the EE of thymol. During drying, thymol migrated upward with the oil droplets, resulting in an increase in thymol loss. Meanwhile, the high content of thymol can reduce the stability of the emulsion system (Robledo et al., 2018). During drying, the high level of

Table 1
Thickness, mechanical properties and water vapor permeability of SPI-based emulsion films.

	Oil (%)	Thickness (μm)	TS (MPa)	EAB (%)	WVP ($\times 10^{-10}$ g·m^{-1}·s^{-1}·Pa^{-1})
	Control (20)	74.00 ± 1.89^{b}	7.56 ± 0.44^{b}	50.08 ± 6.31^{f}	1.34 ± 0.03^{e}
	0	67.67 ± 3.09^{c}	9.23 ± 0.21^{a}	35.89 ± 1.41^{g}	2.72 ± 0.05^{a}
O/W	10	70.95 ± 4.51^{bc}	6.19 ± 0.17^{c}	87.42 ± 7.61^{d}	2.30 ± 0.26^{b}
	20	75.05 ± 1.35^{ab}	5.78 ± 0.12^{d}	82.75 ± 4.83^{d}	2.09 ± 0.07^{b}
	30	79.40 ± 3.23^{a}	5.44 ± 0.12^{de}	68.58 ± 8.09^{e}	1.84 ± 0.11^{c}
HIP	10	71.89 ± 1.50^{bc}	5.78 ± 0.16^{d}	114.70 ± 11.91^{c}	1.72 ± 0.11^{cd}
	20	75.47 ± 3.42^{ab}	5.19 ± 0.17^{e}	139.79 ± 10.19^{b}	1.58 ± 0.13^{d}
	30	79.56 ± 1.59^{a}	4.47 ± 0.19^{f}	160.83 ± 12.96^{a}	1.15 ± 0.12^{e}

Data are expressed as mean ± standard deviation.
Values with different lowercase letters in the same column indicate significant differences at $P < 0.05$.

Table 2
Color and transparency value of SPI-based emulsion films.

	Oil (%)	L^*	a^*	b^*	ΔE	Transparency value
	Control (20)	90.38 ± 0.18^{b}	-1.52 ± 0.03^{c}	9.13 ± 0.15^{d}	7.91 ± 0.12^{e}	5.29 ± 0.19^{f}
	0	91.67 ± 0.12^{a}	-1.37 ± 0.02^{a}	8.49 ± 0.11^{e}	7.09 ± 0.11^{f}	1.00 ± 0.09^{h}
O/W	10	90.13 ± 0.18^{b}	-1.52 ± 0.01^{c}	8.97 ± 0.32^{d}	7.89 ± 0.23^{e}	4.55 ± 0.11^{g}
	20	89.81 ± 0.22^{c}	-1.45 ± 0.05^{b}	9.23 ± 0.20^{d}	8.25 ± 0.01^{d}	6.60 ± 0.11^{e}
	30	89.29 ± 0.05^{d}	-1.44 ± 0.02^{b}	10.61 ± 0.19^{c}	9.56 ± 0.18^{c}	7.12 ± 0.14^{d}
HIP	10	89.54 ± 0.09^{cd}	-1.64 ± 0.05^{d}	10.58 ± 0.11^{c}	9.48 ± 0.09^{c}	7.99 ± 0.18^{c}
	20	88.53 ± 0.17^{e}	-1.63 ± 0.03^{d}	11.57 ± 0.17^{b}	10.71 ± 0.21^{b}	11.19 ± 0.09^{b}
	30	86.34 ± 0.12^{f}	-1.59 ± 0.04^{d}	12.37 ± 0.09^{a}	12.28 ± 0.08^{a}	12.87 ± 0.22^{a}

Data are expressed as mean ± standard deviation.
Values with different lowercase letters in the same column indicate significant differences at $P < 0.05$.

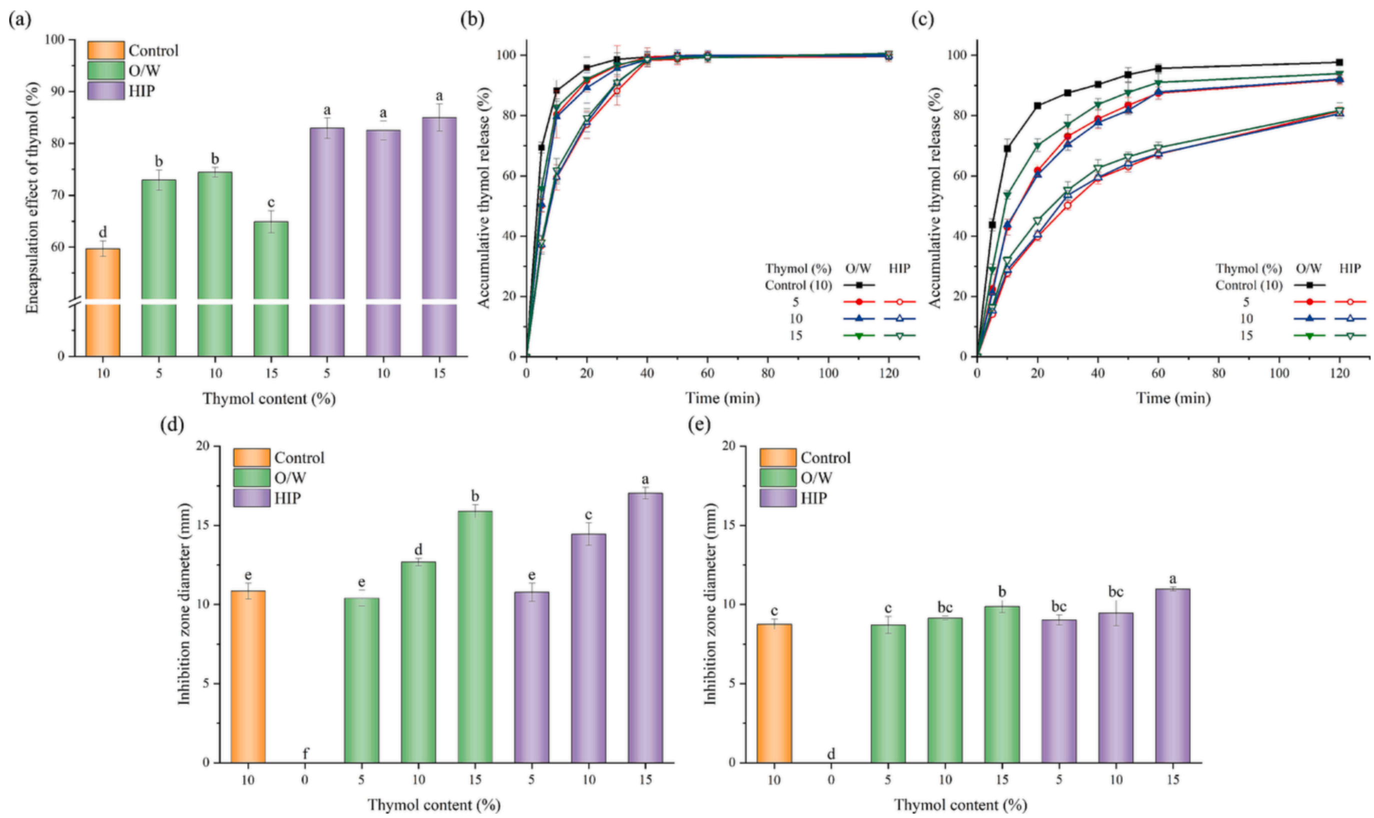

Fig. 4. (a) Encapsulation efficiency of thymol in SPI-based emulsion films; Thymol release properties of SPI-based emulsion films in water (b) and 50% ethanol (c); Growth inhibition effect of SPI-based emulsion film loaded with thymol on *Escherichia coli* (d) and *Staphylococcus aureus* (e).

thymol led to aggregation, resulting in the formation of spherical clusters and disrupting the film integrity (Sharma et al., 2023). Therefore, the reduced EE of thymol was observed in the SPI-based emulsion films with O/W emulsion when the thymol content reached 15 %. By contrast, the EE of thymol remained stable in the SPI-based emulsion films with HIP emulsion with the increasing thymol content. This finding suggested that the SPI-based emulsion films with HIP emulsion have a good EE of thymol because the oil droplets loaded with thymol are distributed in a compact protein network structure.

3.3.2. Thymol release characteristics of SPI-based emulsion films

Thymol was rapidly released within 40 min in the water system as presented in Fig. 4b. In the 50 % (v/v) ethanol system (Fig. 4c), a fast initial release of thymol from the films was observed, followed by a continuous slow release. This phenomenon occurred because the free and semi-free thymol particles cannot be firmly bound in the films (Zhang, et al., 2022). This result was also observed in pectin films containing thymol and chitosan films containing thyme essential oil (Zhang et al., 2022; Lian et al., 2020). The difference in thymol release properties between the films in the water system and 50 % ethanol system can be attributed to the difference in films' swelling. The rapid swelling of the SPI-based emulsion films was founded in the water system (Fig. S2), resulting in easy contact of thymol with solvent molecules. Regardless of the food simulation system, the SPI-based emulsion films with HIP emulsion had the lowest thymol release rate compared with the other SPI-based emulsion films, indicating that the films with HIP emulsion had good sustained antimicrobial ability in the application. This finding was related to the distribution and stability of thymol in the SPI-based emulsion films. On the one hand, thymol could move upward with the migration of oil droplets, allowing its easy release into the solvent system. On the other hand, the thymol loaded into small oil droplets could be evenly distributed in the film, improving the stability of thymol. Thymol content had no effect on the thymol release rate when water was used as the solvent, and this finding was related to the rapid swelling of the films. The thymol release rate increased with the thymol content when 50 % ethanol was used as the solvent. The high content of thymol can reduce the compactness of the film structure (Sharma et al., 2023), especially in the SPI-based emulsion films with O/W emulsion.

3.3.3. Antimicrobial activity of SPI-based emulsion films

As presented in Fig. 4d and e, the incorporation of emulsion loaded with thymol could significantly increase the inhibition effect of SPI films on bacterial growth compared with the control groups ($P < 0.05$). This finding was related to the EE of thymol (Fig. 4a). Moreover, the surfactant can improve the water solubility of the essential oil, allowing them to easily interact with bacteria (Gaysinsky, Davidson, Bruce, & Weiss, 2005). The SPI-based emulsion films with HIP emulsion had a stronger antimicrobial effect on *E. coli* and *S. aureus* than the SPI-based emulsion films with O/W emulsion. The films prepared using HIP emulsion loaded with thymol have a compact protein structure and even distribution of thymol, which improve the EE of thymol in the films and effectively increase the antimicrobial activity of the films. As expected, the antimicrobial activity of the SPI-based emulsion films increased with the thymol incorporation. Moreover, the films exhibited higher antimicrobial activity against *E. coli* than *S. aureus* (Fig. 4d and e) because the cell wall of Gram-positive bacteria is usually formed by several layers of peptidoglycan, which can effectively prevent the penetration of hydrophobic substances and reduce the antimicrobial effect of essential oil on the bacteria (Aman Mohammadi et al., 2021).

4. Conclusion

HIP emulsion could improve the compatibility of oil in the SPI film and enhance the stability of thymol. The FFE prepared with HIP emulsion had the smallest oil droplet size, which improved the anti-coalescence ability of oil droplets during drying and contributed to the formation of SPI-based emulsion films with small and uniformly distributed oil droplets. Therefore, HIP emulsion could significantly reduce the T_g, TS, and WVP of SPI films. The SPI-based emulsion films with HIP emulsion had the highest encapsulation efficiency and best sustained release of thymol due to the excellent oil compatibility, leading to their highest antimicrobial activity. In conclusion, the SPI-based emulsion films with HIP emulsion contained small and highly compatible oil droplets, which are beneficial for preparing films with good thymol sustained release effect and antimicrobial activity.

CRediT authorship contribution statement

Yuan Zhao: Writing – original draft, Methodology, Data curation. **Linfan Shi:** Supervision. **Zhongyang Ren:** Supervision. **Qun Liu:** Supervision. **Yucang Zhang:** Supervision. **Wuyin Weng:** Writing – review & editing, Conceptualization.

Declaration of competing interest

The authors declare that they have no known competing financial interests or personal relationships that could have appeared to influence the work reported in this paper.

Data availability

The authors do not have permission to share data.

Acknowledgements

This work is sponsored by National Natural Science Foundation of China (32272266), National Key R&D Program of China (2021YFD2100200/2021YFD2100204) and Xiamen Science and Technology Project (20221001).

Appendix A. Supplementary data

Supplementary data to this article can be found online at https://doi.org/10.1016/j.fochx.2024.101251.

References

Ajesh, K. V., Hasan, M., Mangaraj, S. M. P., Verma, D. K., & Srivastav, P. P. (2022). Trends in edible packaging films and its prospective future in food: A review. *Applied Food Research, 2*(1), Article 100118. https://doi.org/10.1016/j.afres.2022.100118

Almasi, L., Radi, M., Amiri, S., & McClements, D. J. (2021). Fabrication and characterization of antimicrobial biopolymer films containing essential oil-loaded microemulsions or nanoemulsions. *Food Hydrocolloids, 117*, Article 106733. https://doi.org/10.1016/j.foodhyd.2021.106733

Aman Mohammadi, M., Ramezani, S., Hosseini, H., Mortazavian, A. M., Hosseini, S. M., & Ghorbani, M. (2021). Electrospun antibacterial and antioxidant zein/polylactic acid/hydroxypropyl methylcellulose nanofibers as an active food packaging system. *Food and Bioprocess Technology, 14*(8), 1529–1541. https://doi.org/10.1007/s11947-021-02654-7

Bai, Y., Qiu, T., Chen, B., Shen, C., Yu, C., Luo, Z., et al. (2023). Formulation and stabilization of high internal phase emulsions: Stabilization by cellulose nanocrystals and gelatinized soluble starch. *Carbohydrate Polymers, 312*, Article 120693. https://doi.org/10.1016/j.carbpol.2023.120693

Dag, D., Jung, J., & Zhao, Y. (2023). Development and characterization of cinnamon essential oil incorporated active, printable and heat sealable cellulose nanofiber reinforced hydroxypropyl methylcellulose films. *Food Packaging and Shelf Life, 39*, Article 101153. https://doi.org/10.1016/j.fpsl.2023.101153

Fattahi, R., & Seyedain-Ardabili, M. (2021). A comparative study on the effect of homogenization conditions on the properties of the film-forming emulsions and the resultant films. *Food Chemistry, 352*, Article 129319. https://doi.org/10.1016/j.foodchem.2021.129319

Galus, S. (2018). Functional properties of soy protein isolate edible films as affected by rapeseed oil concentration. *Food Hydrocolloids, 85*, 233-241. https://doi.org/10.1016/j.foodhyd.2018.07.026.

Gao, H., Ma, L., Cheng, C., Liu, J., Liang, R., Zou, L., et al. (2021). Review of recent advances in the preparation, properties, and applications of high internal phase emulsions. *Trends in Food Science & Technology, 112*, 36–49. https://doi.org/10.1016/j.tifs.2021.03.041

Gaysinsky, S., Davidson, P. M., Bruce, B. D., & Weiss, J. (2005). Growth inhibition of escherichia coli O157:H7 and listeria monocytogenes by carvacrol and eugenol encapsulated in surfactant micelles. *Journal of Food Protection, 68*(12), 2559–2566. https://doi.org/10.4315/0362-028X-68.12.2559

Hosseini, S. F., Mousavi, Z., & McClements, D. J. (2023). Beeswax: A review on the recent progress in the development of superhydrophobic films/coatings and their applications in fruits preservation. *Food Chemistry, 424*, Article 136404. https://doi.org/10.1016/j.foodchem.2023.136404

Hu, X., Binks, B. P., & Cui, Z. (2021). High internal phase emulsions stabilized by adsorbed sucrose stearate molecules and dispersed vesicles. *Food Hydrocolloids, 121*, Article 107002. https://doi.org/10.1016/j.foodhyd.2021.107002

Hu, Y., Xu, W., Ren, Z., Shi, L., Zhang, Y., Yang, S., et al. (2023). Effect of drying rate on the physicochemical properties of soy protein isolate-soy oil emulsion films. *Food Packaging and Shelf Life, 36*, Article 101038. https://doi.org/10.1016/j.fpsl.2023.101038

Hu, Y., Yang, S., Zhang, Y., Shi, L., Ren, Z., Hao, G., et al. (2022). Effects of microfluidization cycles on physicochemical properties of soy protein isolate-soy oil emulsion films. *Food Hydrocolloids, 130*, Article 107684. https://doi.org/10.1016/j.foodhyd.2022.107684

Jorge, A. M. S., Gaspar, M. C., Henriques, M. H. F., & Braga, M. E. M. (2023). Edible films produced from agrifood by-products and wastes. *Innovative Food Science & Emerging Technologies, 88*, Article 103442. https://doi.org/10.1016/j.ifset.2023.103442

Kaewprachu, P., Ben Amara, C., Oulahal, N., Gharsallaoui, A., Joly, C., Tongdeesoontorn, W., et al. (2018). Gelatin films with nisin and catechin for minced pork preservation. *Food Packaging and Shelf Life, 18*, 173–183. https://doi.org/10.1016/j.fpsl.2018.10.011

Li, R., Xue, H., Gao, B., Liu, H., Han, T., Hu, X., et al. (2022). Physicochemical properties and digestibility of thermally induced ovalbumin–oil emulsion gels: Effect of interfacial film type and oil droplets size. *Food Hydrocolloids, 131*, Article 107747. https://doi.org/10.1016/j.foodhyd.2022.107747

Li, X., Shen, Y., Hu, F., Zhang, X., Thakur, K., Rengasamy, K. R. R., et al. (2023a). Fortification of polysaccharide-based packaging films and coatings with essential oils: A review of their preparation and use in meat preservation. *International Journal of Biological Macromolecules, 242*, Article 124767. https://doi.org/10.1016/j.ijbiomac.2023.124767

Li, X., Sha, X., Yang, H., Ren, Z., & Tu, Z. (2023b). Ultrasonic treatment regulates the properties of gelatin emulsion to obtain high-quality gelatin film. *Food Chemistry: X, 18*, Article 100673. https://doi.org/10.1016/j.fochx.2023.100673

Lian, H., Shi, J., Zhang, X., & Peng, Y. (2020). Effect of the added polysaccharide on the release of thyme essential oil and structure properties of chitosan based film. *Food Packaging and Shelf Life, 23*, Article 100467. https://doi.org/10.1016/j.fpsl.2020.100467

Liang, Q., & Gao, Q. (2023). Effect of amylose content on the preparation for carboxymethyl starch/pullulan electrospun nanofibers and their properties as encapsulants of thymol. *Food Hydrocolloids, 136*, Article 108250. https://doi.org/10.1016/j.foodhyd.2022.108250

Ozulku, G., Yildirim, R. M., Toker, O. S., Karasu, S., & Durak, M. Z. (2017). Rapid detection of adulteration of cold pressed sesame oil adultered with hazelnut, canola, and sunflower oils using ATR-FTIR spectroscopy combined with chemometric. *Food Control, 82*, 212–216. https://doi.org/10.1016/j.foodcont.2017.06.034

Pateiro, M., Munekata, P. E. S., Sant'Ana, A. S., Domínguez, R., Rodríguez-Lázaro, D., & Lorenzo, J. M. (2021). Application of essential oils as antimicrobial agents against spoilage and pathogenic microorganisms in meat products. *International Journal of*

Food Microbiology, 337, Article 108966. https://doi.org/10.1016/j.ijfoodmicro.2020.108966

Rani, P., Yu, X., Liu, H., Li, K., He, Y., Tian, H., et al. (2021). Material, antibacterial and anticancer properties of natural polyphenols incorporated soy protein isolate: a review. *European Polymer Journal, 152*, Article 110494. https://doi.org/10.1016/j.eurpolymj.2021.110494

Rashid, A., Qayum, A., Liang, Q., Kang, L., Raza, H., Chi, Z., et al. (2023). Preparation and characterization of ultrasound-assisted essential oil-loaded nanoemulsions stimulated pullulan-based bioactive film for strawberry fruit preservation. *Food Chemistry, 422*, Article 136254. https://doi.org/10.1016/j.foodchem.2023.136254

Robledo, N., Vera, P., López, L., Yazdani-Pedram, M., Tapia, C., & Abugoch, L. (2018). Thymol nanoemulsions incorporated in quinoa protein/chitosan edible films; antifungal effect in cherry tomatoes. *Food Chemistry, 246*, 211–219. https://doi.org/10.1016/j.foodchem.2017.11.032

Sedaghat Doost, A., Van Camp, J., Dewettinck, K., & Van der Meeren, P. (2019). Production of thymol nanoemulsions stabilized using quillaja saponin as a biosurfactant: Antioxidant activity enhancement. *Food Chemistry, 293*, 134–143. https://doi.org/10.1016/j.foodchem.2019.04.090

Shao, L., Xi, Y., & Weng, Y. (2022). Recent advances in PLA-based antibacterial food packaging and its applications. *Molecules, 27*, 5953. https://doi.org/10.3390/molecules27185953

Sharma, K., Munjal, M., Sharma, R. K., & Sharma, M. (2023). Thymol encapsulated chitosan-Aloe vera films for antimicrobial infection. *International Journal of Biological Macromolecules, 235*, Article 123897. https://doi.org/10.1016/j.ijbiomac.2023.123897

Shen, G., Yu, G., Wu, H., Li, S., Hou, X., Li, M., et al. (2022). Incorporation of lipids into wheat bran cellulose/wheat gluten composite film improves its water resistance properties. *Membranes, 12*, 18. https://doi.org/10.3390/membranes12010018

Tongnuanchan, P., Benjakul, S., & Prodpran, T. (2014). Structural, morphological and thermal behaviour characterisations of fish gelatin film incorporated with basil and citronella essential oils as affected by surfactants. *Food Hydrocolloids, 41*, 33–43. https://doi.org/10.1016/j.foodhyd.2014.03.015

Wang, M., Li, Y. C., Meng, F. B., Wang, Q., Wang, Z. W., & Liu, D. Y. (2023). Effect of honeysuckle leaf extract on the physicochemical properties of carboxymethyl konjac glucomannan/konjac glucomannan/gelatin composite edible film. *Food Chemistry: X, 18*, Article 100675. https://doi.org/10.1016/j.fochx.2023.100675

Xu, J., He, M., Wei, C., Duan, M., Yu, S., Li, D., et al. (2023). Konjac glucomannan films with Pickering emulsion stabilized by TEMPO-oxidized chitin nanocrystal for active food packaging. *Food Hydrocolloids, 139*, Article 108539. https://doi.org/10.1016/j.foodhyd.2023.108539

Xue, F., Gu, Y. C., Wang, Y., Li, C., & Adhikari, B. (2019). Encapsulation of essential oil in emulsion based edible films prepared by soy protein isolate-gum acacia conjugates. *Food Hydrocolloids, 96*, 178–189. https://doi.org/10.1016/j.foodhyd.2019.05.014

Zhang, L., Zhang, M., Mujumdar, A. S., Wang, D., & Ma, Y. (2023). Novel multilayer chitosan/emulsion-loaded syringic acid grafted apple pectin film with sustained control release for active food packaging. *Food Hydrocolloids, 142*, Article 108823. https://doi.org/10.1016/j.foodhyd.2023.108823

Zhang, W., Cao, J., & Jiang, W. (2022). Effect of different cation in situ cross-linking on the properties of pectin-thymol active film. *Food Hydrocolloids, 128*, Article 107594. https://doi.org/10.1016/j.foodhyd.2022.107594

Zhang, X., Ismail, B. B., Cheng, H., Jin, T. Z., Qian, M., Arabi, S. A., et al. (2021). Emerging chitosan-essential oil films and coatings for food preservation - a review of advances and applications. *Carbohydrate Polymers, 273*, Article 118616. https://doi.org/10.1016/j.carbpol.2021.118616

Zhao, Y., Ren, Z., Shi, L., Zhang, Y., & Weng, W. (2023a). Effects of pre-emulsion prepared using sucrose esters with different hydrophile-lipophile balances on characteristics of soy protein isolate emulsion films. *Food Research International, 165*, Article 112542. https://doi.org/10.1016/j.foodres.2023.112542

Zhao, Y., Ren, Z., Shi, L., & Weng, W. (2023b). Effect of W/O pre-emulsion prepared with different emulsifiers on the physicochemical properties of soy protein isolate-based emulsion films. *Food Hydrocolloids, 139*, Article 108440. https://doi.org/10.1016/j.foodhyd.2022.108440

Zhou, R., Zhao, Y., Ren, Z., Shi, L., Zhang, Y., & Weng, W. (2023). Physicochemical properties of soybean β-conglycinin-based films affected by linoleic acid. *Food Chemistry: X, 17*, Article 100609. https://doi.org/10.1016/j.fochx.2023.100609

Zhou, X., Zong, X., Wang, S., Yin, C., Gao, X., Xiong, G., et al. (2021). Emulsified blend film based on konjac glucomannan/carrageenan/ camellia oil: Physical, structural, and water barrier properties. *Carbohydrate Polymers, 251*, Article 117100. https://doi.org/10.1016/j.carbpol.2020.117100